Cancer Letters 361 (2015) 251–261

Contents lists available at ScienceDirect

Cancer Letters

journal homepage: www.elsevier.com/locate/canlet

Original Articles

Antiproliferative activity of the isoindigo 5′-Br in HL-60 cells is mediated by apoptosis, dysregulation of mitochondrial functions and arresting cell cycle at G0/G1 phase

Ayman M. Saleh [a,b,*], Mustafa M. El-Abadelah [c], Mohammad Azhar Aziz [b], Mutasem O. Taha [d], Amre Nasr [a,e], Syed A.A. Rizvi [f]

[a] Department of Basic Medical Sciences, College of Medicine, King Saud Bin Abdulaziz University for Health Sciences (KSAU-HS), National Guard Health Affairs, P.O. Box: 3660, Mail Code: 3127, Riyadh 11481, Saudi Arabia
[b] King Abdullah International Medical Research Center (KAIMRC), National Guard Health Affairs, P.O. Box 22490, Riyadh 11426, Saudi Arabia
[c] Department of Chemistry, Faculty of Science, The University of Jordan, Amman 11942, Jordan
[d] Department of Pharmaceutical Sciences, Faculty of Pharmacy, The University of Jordan, Amman 11942, Jordan
[e] Department of Microbiology, Faculty of Sciences and Technology, Al-Neelain University, Khartoum, Sudan
[f] Department of Pharmaceutical Sciences, College of Pharmacy, Nova Southeastern University (NSU), Fort Lauderdale, Florida 33328, USA

ARTICLE INFO

Article history:
Received 10 February 2015
Received in revised form 9 March 2015
Accepted 10 March 2015

Keywords:
Isoindigo
Anticancer
Apoptosis
Mitochondria dysfunction
Cell cycle
CDK

ABSTRACT

Our new compound, 5′-Br [(*E*)-1-(5′-bromo-2′-oxoindolin-3′-ylidene)-6-ethyl-2,3,6,9-tetrahydro-2,9-dioxo-1*H*-pyrrolo[3,2-*f*]quinoline-8-carboxylic acid], had shown strong, selective antiproliferative activity against different cancer cell lines. Here, we aim to comprehensively characterize the mechanisms associated with its cytotoxicity in the human promyelocytic leukemia HL-60 cells. We focused at studying the involvement of apoptotic pathway and cell cycle effects. 5′-Br significantly inhibited proliferation by inducing caspase-dependent apoptosis. Involvement of caspase independent mechanism is also possible due to observed inability of z-VAD-FMK to rescue apoptotic cells. 5′-Br was found to trigger intrinsic apoptotic pathway as indicated by depolarization of the mitochondrial inner membrane, decreased level of cellular ATP, modulated expression and phosphorylation of Bcl-2 leading to loss of its association with Bax, and increased release of cytochrome *c*. 5′-Br treated cells were found arrested at G0/G1 phase with modulation in protein levels of cyclins, dependent kinases and their inhibitors. Expression and enzymatic activity of CDK2 and CDK4 was found inhibited. Retinoblastoma protein (Rb) phosphorylation was also inhibited whereas p21 protein levels were increased. These results suggest that the antiproliferative mechanisms of action of 5′-Br could involve apoptotic pathways, dysregulation of mitochondrial functions and disruption of cell cycle checkpoint.

Introduction

Acute myeloid leukemia (AML) is hematopoietic malignancy characterized by uncontrolled proliferation and accumulation of myeloblasts in the bone marrow, blood, and other organs [1]. This complex disease involves multiple genetic and molecular alterations causing cellular transformation, deregulation of apoptosis, proliferation, invasion, angiogenesis and metastasis [1]. AML patients typically respond to initial treatment with anthracycline and cytarabine (1-β-*D*-Arabinofuranosylcytosine, Ara-C)-based chemotherapy, however, the response is poor or short-lived and often associated with relapse and resistance. The inadequacy of conventionally available therapies in AML has fueled the quest for finding new molecules that can be used in chemotherapy with better selectivity and efficacy.

The bis-indole containing alkaloids indigo, indirubin and isoindigo have been employed in treating myeloid leukemia. The clinical application of these drugs in treating myeloid leukemia is hampered by their potential side effects, poor water solubility, bone marrow suppression and drug-resistance in prolonged treatments [2]. In addition, the limited water solubility of these isoindigos hinders the

Abbreviations: 5′-Br, [(*E*)-1-(5′-bromo-2′-oxoindolin-3′-ylidene)-6-ethyl-2,3,6,9-tetrahydro-2,9-dioxo-1*H*-pyrrolo[3,2-*f*]quinoline-8-carboxylic acid]; ΔΨm, difference in mitochondrial transmembrane potential; Bcl-2, B-cell lymphoma 2; Bcl-xL, B-cell lymphoma-extra-large; Bax, Bcl-2-associated X protein; Bak, Bcl-2 homologous antagonist killer; PARP, poly (ADP-ribose) polymerase; CDK, cyclin dependent kinase; CKI, cyclin kinase inhibitor; Rb, retinoblastoma protein; z-VAD-FMK, *N*-benzyloxycarbonyl-Val-Ala-Asp-fluoromethyl ketone; Ac-LEHD-pNA, *N*-acetyl-Leu-Glu-His-Asp-*p*-nitroanilide; Ac-IETD-pNA, *N*-acetyl-Ile-Glu-Thr-Asp-*p*-nitroanilide; Ac-DEVD-*p*NA, *N*-acetyl-Asp-Glu-Val-Asp-*p*-nitroanilide; Ac-VDVAD, *N*-acetyl-Val-Asp-Val-Ala-Asp-p-nitroanilide; Ac-VEID-pNA, *N*-acetyl-Val-Glu-Ile-Asp-p-nitroanilide; pNA, p-nitroanilide; DMSO, dimethyl sulfoxide.

* Corresponding author. Tel.: +966 11 429 95268; fax: +966 11 429 95276.
E-mail addresses: salehay@ksau-hs.edu.sa; salehay@ngha.med.sa (A.M. Saleh).

http://dx.doi.org/10.1016/j.canlet.2015.03.013

detailed characterization of their antiproliferative signaling pathways. Thus, extensive efforts have been employed to synthesize novel indirubin and isoindigo derivatives with increased bioavailability and bioactivity. In spite of the extensive investigations for the mode of action of isoindigos in myeloid leukemia and other cancers, there are gaps in our understanding of their cellular targets and mechanism of action.

The antileukemic effects of these compounds are mediated through multi-signaling pathways including inhibition of DNA biosynthesis and assembly of microtubules, arresting cells at G1 phase of the cell cycle, interaction with the aryl hydrocarbon receptor (AhR) triggering cell differentiation and maturation leading to complete inhibition of cell growth, and down-regulation of *c-myb* gene expression [2–6]. Several of these compounds have been shown to inhibit cyclin-dependent kinases (CDKs) and glycogen-synthase kinase (GSK-3β), and induce apoptosis with varying degrees of potency [2–5,7–12]. Recently, a novel 7-azaisoindigo derivative [namely N(1)-(*n*-butyl)-7-azaisoindigo] has been shown to trigger apoptosis through reactive oxygen species (ROS), deregulation of the mitochondrial functions and activation of caspases [13].

Successful chemotherapeutics are able to trigger death of cancer cells mainly through intrinsic/extrinsic apoptotic pathways [14]. Apart from extrinsic apoptotic pathway that is dependent on a receptor-mediated activation of caspase-8, these drugs may stimulate the intrinsic (mitochondria-dependent) pathway which is evoked by the release of mitochondrial apoptogenic factors such as cytochrome c to the cytosol allowing activation of caspase-9 [15].

Tumor cells are characterized by having a deregulated cell cycle, which contributes to their uncontrolled proliferation (reviewed in Refs. 16 and 17). The molecular mechanisms of cell cycle arrest by many anticancer agents involve modulation of several cell cycle regulatory proteins. Although human cells highly express the D type cyclins (D1, D2 and D3) in early and late G1 phase [18–20], proper execution of later phases (S and G2-M) require the subsequent activation of other CDK-cyclin complexes: CDK2/cyclin E, CDK2/cyclin A, CDK1/cyclin A and CDK1/cyclin B [16,21]. CDK activity can be regulated by cell cycle inhibitory proteins (CKI), which bind to CDK alone or to the CDK/cyclin complex [16,17].

In line with the efforts aiming to synthesize more soluble and effective anticancer isoindigo derivatives, we have identified a compound [(*E*)-1-(5′-bromo-2′-oxoindolin-3′-ylidene)-6-ethyl-2,3,6,9-tetrahydro-2,9-dioxo-1*H*-pyrrolo[3,2-*f*]quinoline-8-carboxylic acid] (known here as 5′-Br, Fig. 1A) with increased solubility (up to 25 mM) in 25% aqueous DMSO (dimethyl sulphoxide) [22]. 5′-Br effectively inhibited the proliferation of several human hematological and solid tumor cell lines at low doses in a selective manner [22].

The acute promyelocytic leukemia cell line HL-60 is a subtype of AML, which accounts for approximately 10% of all AML cases [1]. Therefore, it is an ideal cell line to investigate novel potential chemotherapeutic agents for this subtype of AML. In this report, we studied the effect of 5′-Br in triggering apoptosis and cell cycle effects in HL-60 cells. Evidence suggests that 5′-Br induces mitochondrial apoptosis in HL-60 cells. 5′-Br triggers depolarization of mitochondria in HL-60 cells, decreases the expression of the anti-apoptotic protein Bcl-2 and promotes its hyperphosphorylation leading to loss of functional association with the proapoptotic factor Bax. The antiproliferative effect is also shown to be through G0/G1 phase arrest, which is mediated by modulating the expression and functions of the G1 phase-related proteins. 5′-Br inhibited expression of cyclin D1 and D2, and reduced Rb phosphorylation. It also significantly upregulated expression of p21 and inhibited expression levels as well as activities of CDK2 and CDK4. These results suggest that the cytotoxic and antiproliferative effects of 5′-Br are mediated by apoptosis, dysregulation of mitochondria functions and cell cycle checkpoint regulation.

Materials and methods

Reagents

The pyridone-annelated isoindigo 5′-Br compound [(*E*)-1-(5′-bromo-2′-oxoindolin-3′-ylidene)-6-ethyl-2,3,6,9-tetrahydro-2,9-dioxo-1*H*-pyrrolo[3,2-*f*]quinoline-8-carboxylic acid] was previously synthesized and chemically characterized in details in our recent publication [22]. Other reagents and experimental protocols used in this study are provided in Supplementary Methods.

Cell viability assay

The quantitative determination of viable cells after various treatments was performed by using the dual DNA intercalating fluorescent dyes kit from EMD Millipore Bioscience (Muse™ Cell Count & Viability Assay). Briefly, 3×10^5 of HL-60, in a 1.0 mL of RPMI-1640 medium, was seeded in each well of a 24 well-plate. After 24 hr, cells were exposed to increasing concentrations of 5′-Br (0.0–16.0 μM) for additional 24 hr. Alternatively, HL-60 cells were incubated with 8.0 μM 5′-Br for different time-points (0–72 hr) before analysis. Cytarabine (0.01–0.03 μM) was added to HL-60 cells as positive controls.

Analysis of apoptosis by flow cytometry

The percentage of cells undergoing apoptosis after treatment with 5′-Br was determined using the Muse™ Annexin-V and Dead Cell Assay kit (EMD Millipore Bioscience) and Muse™ cell analyzer according to the manufacturer's protocol. The kit utilizes a fluorescent dye (FITC) conjugated to Annexin-V to detect phosphatidylserine (PS) on the external membrane of apoptotic cells and 7-AAD (7-amino-actinomycin D) as a dead cells marker. When z-VAD-FMK was used, cells were incubated with the desired concentration of this caspase inhibitor for 4 hr before addition of 5′-Br. HL-60 cells were also treated with 0.02 μM cytarabine as positive control.

Analysis of changes in mitochondrial transmembrane potential

Measurement of changes in mitochondria membrane potential ($\Delta\Psi m$) was performed with the Muse™ MitoPotential Assay kit (EMD Millipore Bioscience). This flow cytometry-based assay differentiates 4 populations of cells: live cells with depolarized mitochondrial membrane; MitoPotential$^-$/7-AAD$^-$, live cells with intact mitochondrial membrane; MitoPotential$^+$/7-AAD$^-$, dead cells with depolarized mitochondrial membrane; MitoPotential$^+$/7-AAD$^+$ and dead cells with intact mitochondrial membrane; MitoPotential$^-$/7-AAD$^+$. After treatment with 5′-Br, HL-60 cells were incubated with the fluorescent dyes and the percentage of depolarized cells (depolarized alive + depolarized dead) were determined by Muse™ Cell Analyzer.

Quantitation of ATP levels in HL-60 treated Cells

ATP contents were determined using the ATP Colorimetric/Fluorometric Assay Kit (BioVision, Inc.) according to the manufacturer's instructions. After treatment with 8.0 μM 5′-Br for increasing time points, HL-60 (1×10^6) cells were lysed in a lysis buffer, deproteinized and 10 μL of the supernatant was added to a 50 μL of the assay reaction mixture. Absorbance was measured at OD 570 nm in a Spectra Max™ micro-plate reader. All samples were measured in triplicates and the values were expressed relative to the untreated control.

Release of cytochrome c *from mitochondria to the cytosol of HL-60 cells*

Mitochondrial and cytosolic fractions from HL-60 cells treated with 5′-Br were prepared by differential centrifugation at 4 °C as described in our recent publication [23]. The release of cytochrome *c* from mitochondria into the cytoplasm of 5′-Br-treated HL-60 cells was detected by Western blotting of mitochondrial (30 μg) or cytosolic (50 μg) fractions as previously described [23].

Immunoprecipitation and western blot analyses

For immunoprecipitation, 25×10^6 HL-60 were treated with or without 5′-Br for 24 hr. Cells were lysed in ice-cold lysis buffer containing 20 mM Tris–HCl pH 7.4, 150 mM NaCl, 1 mM EDTA, 0.5% NP-40, and protease inhibitors [2 μg/mL leupeptin, 2 μg/mL aprotinin, 2 μg/mL pepstatin A and 1 mM PMSF]. After centrifugation at 14,000 *g* for 20 min at 4 °C, lysates (300 μg) were pre-cleared by incubating (2 hr at 4 °C) with 25 μL protein A/G plus-agarose beads (Santa Cruz Biotechnology). Pre-cleared lysates were incubated overnight with 5 μg of specific anti-Bax or anti-Bcl-2 antibodies. Immunocomplexes were captured with 25 μL protein A/G plus-agarose, and the presence of Bcl-2 in these complexes was determined by Western blot analysis.

Samples preparation and Western blot analysis were performed as previously described [23]. Primary antibodies against caspase-2 [(C2) Mouse mAb 2224], caspase-8 [(1C12) Mouse mAb 9746], caspase-9 [(C9) Mouse mAb 9508], cleaved caspase-3 [(Asp175) (5A1E) Rabbit mAb 9664], cleaved caspase-6 [(Asp162) Antibody 9761], phospho-Bcl-2 [antibody 2875] and PARP [antibody 9542] were Obtained

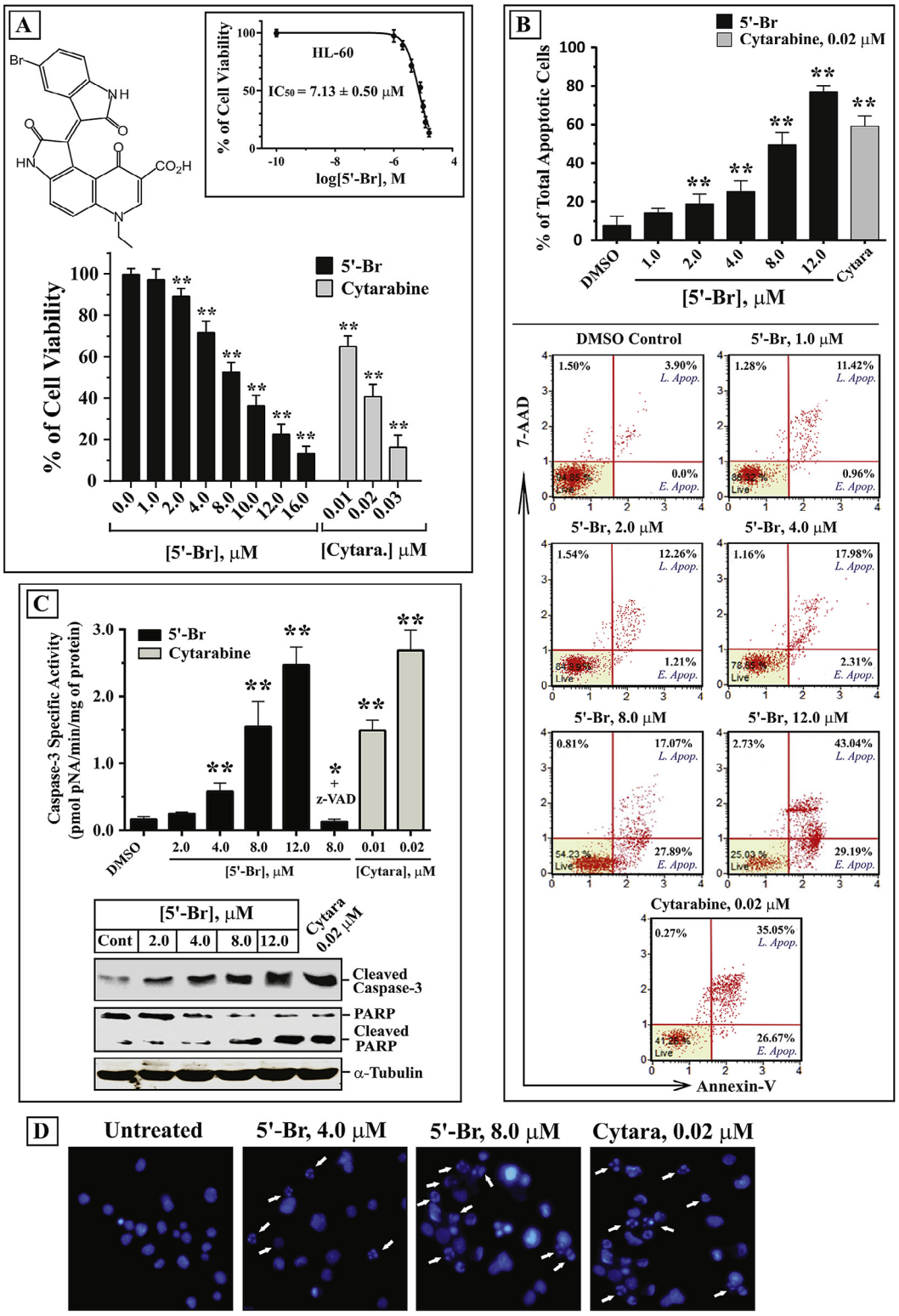

Fig. 1. The antiproliferative activity of 5′-Br is mediated by apoptosis. (A) Clockwise; the chemical structure of 5′-Br [(*E*)-1-(5′-bromo-2′-oxoindolin-3′-ylidene)-6-ethyl-2,3,6,9-tetrahydro-2,9-dioxo-1*H*-pyrrolo[3,2-*f*]quinoline-8-carboxylic acid]. Determination of IC_{50} value: The sigmoidal curve shown was obtained by plotting the mean percentages of viability versus logarithmic molar concentrations of 5′-Br, and the IC_{50} value (7.13 μM) was determined using a non-linear regression analysis of GraphPad Prism 6 software. Dose dependent decrease in cell viability: HL-60 cells were treated with increasing concentrations of 5′-Br (0.0–16.0 μM), or cytarabine (0.0–0.03 μM) for 24 hr. The percentage of cell viability was expressed relative to untreated control containing the carrier solvent DMSO. (B) 5′-Br increases apoptosis in a dose dependent manner: HL-60 cells were treated with varying concentrations of 5′-Br (0.0–12.0 μM) or with 0.02 μM cytarabine for 24 hr and apoptosis was analyzed. The graph represents the summary mean percentages ± SD of apoptosis (early and late apoptosis) of three independent experiments. Bottom panel shows scatter plots representing percentages of early and late apoptosis for one experiment. (C) Caspase-3 activity is increased by 5′-Br: Lysates from HL-60 cells, treated with varying concentrations of 5′-Br, were analyzed for caspase-3 catalytic activity. Caspase 3 activity was completely suppressed by z-VAD-FMK. Increase in cleaved caspase-3 and cleaved PARP levels were observed by Western blotting. (D) Condensation of chromatin material and fragmentation of nuclei in apoptotic cells: HL-60 cells were treated with 5′-Br or cytarabine for 24 hr and stained with Hoechst 33342.

from Cell Signaling Technologies and used in 1:1000 dilution in PBST solution containing 3% bovine serum albumin (BSA). Primary antibodies against Bcl-2 [(C-2): mAb 7382], Bcl-X_L [(H-5): mAb 8392], Bax [(N-20): rAb 493] and Bak [(G-23): rAb 832] (from Santa Cruz Biotechnology) were used in 1:1500 dilution PBST solution containing 5% BSA. Detection of protein of interest was accomplished with secondary antibodies conjugated to horseradish peroxidase and Pierce ECL Plus substrate solution (Thermo Scientific, Rockford, Illinois, USA). Pre-stained protein molecular weight markers (Santa Cruz Biotechnology) were included in each gel. To confirm equal loading of proteins in gels, the blots were also immunoprobed with an antibody against α-tubulin [(H-300): rAb 5546] or β-actin [(C4): mAb 47778] from Santa Cruz Biotechnology.

Flow cytometry analysis of cell cycle

Distribution of cell cycle was analyzed by flow cytometry using the Muse™ Cell Cycle Kit from EMD Millipore Bioscience. The cell cycle analysis was performed according to the manufacturer's protocol, and as recently described [24]. Briefly, exponentially growing HL-60 cells (5×10^5 cells/mL) were treated with different concentrations of 5′-Br (0.0–12.0 μM) for 24 hr or with 8.0 μM for various periods of time (0–48 hr). The range of the selected concentrations was based on the demonstrated IC_{50} for the compound in HL-60 cells (7.13 ± 0.50 μM). After incubation, 1×10^6 cells were harvested, washed with PBS and fixed with ice-cold 70% ethanol at –20 °C for 3 hr. The cells were then washed with PBS, stained with 200 μL of PI/RNAse reagent for 30 min and analyzed by the Muse™ Cell Analyzer. Adherent cells were trypsinized after treatment, washed once with PBS, and fixed in 70% ethanol overnight at –20 °C before analysis as described earlier. All the compound stock solutions were prepared in a solvent containing 50% DMSO and 50% PBS. Therefore, the control cells were treated with equal amount of the carrier solvent (0.05% DMS0), and showed no effect on cell cycle when compared with the solvent-free control cells.

CDK2 and CDK4 kinase assay in cell-free systems and in cultured cells

Kinase assays were performed on HL-60 as previously described [25,26], with some modifications. For *in vitro* (cell free system) CDKs kinase assay, exponentially growing untreated HL-60 cells were lysed for 30 min at 4 °C in the lysis buffer. The cell lysate was cleared by centrifugation at 14,000 *g* for 10 min at 4 °C. Protein lysates were pre-cleared twice with 50 μL protein A/G plus-agarose beads. A total of 4 mg of protein was incubated with anti-CDK2 or anti-CDK4 antibody and protein A/G plus agarose for 12 hr at 4 °C. The immunoprecipitates were washed three times with the lysis buffer and twice with a kinase buffer [50 mM HEPES (pH 7.0), 10 mM $MgCl_2$, 5 mM $MnCl_2$, 1 mM DTT, 5 μM ATP] and separated into 10 tubes. The kinase reactions were done in a final volume of 40 μL kinase buffer containing 2 μg histone H1 (for CDK2; Calbiochem, California, USA) or 1 μg Gst-Rb (for CDK4; Santa Cruz Biotechnology) substrates, various concentrations of the test compound, 20 μM unlabeled ATP and 5 μCi [γ-^{32}P]ATP (3000 Ci/mmol, PerkinElmer Inc., Waltham, MA, USA), and carried out for 30 min at 30 °C. SDS sample buffer was then added and the mixtures were then boiled for 5 min, and protein was separated on 12% polyacrylamide gels. The gels were dried, visualized by autoradiography, and the bands were quantitated by densitometry.

For *in vivo* CDKs kinase assay in 5′-Br-treated cell, HL-60 cells (3×10^5/mL) were seeded in 100 mm plastic culture dishes for 24 hr and subsequently treated with different concentrations of 5′-Br (0–12.0 μM) for 24 hr or with a fixed concentration of 8.0 μM for various periods of time (0–48 hr). Cell lysis preparation and immunoprecipitation were performed as described earlier. Kinase assay was carried out in 50 μL kinase buffer with CDK2- or CDK4-immunoprecipitates from 300 μg of protein lysate. Before addition of the radioactive ATP, 10 μL of the slurry was removed from each sample to separate tubes for Western blot analysis of the immunoprecipitated CDK, to verify that equal amount of the desired CDK is present in each sample. To the remaining 40 μL, 5 μCi [γ-^{32}P]ATP was added to each reaction tube and the kinase assay was performed as described earlier.

Statistical analysis

Data presented are the means ± SD of results from a minimum of three independent experiments with similar patterns unless otherwise mentioned. Statistical analysis was performed using one-way ANOVA, and Tukey–Kramer multiple-comparison test was performed by using GraphPad Prism 6 software. A $p < 0.05$ value was considered statistically significant.

Results

5′-Br inhibits the proliferation of HL-60 cells by apoptosis

5′-Br inhibited the proliferation of HL-60 cells in a dose and time dependent manner. The cell viability decreased from 89.23 ± 3.24% at a concentration of 2.0 μM to 22.6 ± 4.23% at 12.0 μM, with an IC_{50} of 7.13 ± 0.5 μM (Fig. 1A). 5′-Br (8.0 μM) inhibited the growth of HL-60 cells in a time-dependent manner with >50% loss in cell viability within 24 hr (Supplementary Fig. S1A). Dose dependent increase in the percentage of apoptotic cells from 14.24 ± 2.21% to 77.10 ± 3.00% after treatment with 1.0–12.0 μM of the compound was observed (Fig. 1B). Induction of apoptosis was time-dependent as shown by 70% increase in apoptotic cells (from 6.50 ± 3.54% to 76.50 ± 9.20%) after treatment for 72 hr (Supplementary Fig. S1B). The annexin-V/7-AAD results coincide with the demonstrated effect by viability assay, and suggest that most of antiproliferative activity of 5′-Br is mediated by apoptosis. Induction of late apoptotic events were reflected by activation of terminal caspase-3 and detection of cleaved PARP (Fig. 1C), along with condensation of the chromatin material/fragmentation of nuclei (Fig. 1D) in a dose dependent manner showing maximum response at 12.0 μM.

5′-Br induced apoptosis could be partially dependent on caspase activation

In addition to caspase-3, the effect of 5′-Br involved caspases-2, -8, -9 and -6 as exhibited by increase in their specific activity and generation of cleaved products in a dose dependent manner. As shown in Supplementary Fig. S2A, 5′-Br was found to trigger a dose dependent increase in the specific activities of the initiator caspase-2, -8 and -9, and the effector caspase-6. Processing of initiator caspase-2, -8 and -9 were demonstrated by the decrease in the levels of procaspase forms and the appearance of their corresponding cleaved bands (Supplementary Fig. S2B), while the effector caspase-3 and -6 by the increase in the level of the small subunits of the active enzymes (Fig. 1C and Supplementary Fig. S2B).

To further validate 5′-Br-induced caspase dependent apoptosis in HL-60 cells, we analyzed the cell death triggered by the compound in the presence of the general caspase inhibitor z-VAD-FMK (Fig. 2). While the presence of 40.0 μM of z-VAD-FMK was adequate to completely inhibit the 5′-Br-induced activation of all the tested caspases (Fig. 1C and Supplementary Fig. S2A), it caused only ~31% cells to be relieved of apoptosis (Fig. 2). These results indicate that the 5′-Br-induced apoptosis could be, at least in part, dependent on caspase activation.

Role of mitochondria in 5′-Br-induced apoptosis in HL60 cells

In response to 5′-Br treatment, HL-60 cells were found to demonstrate a dose and time dependent increase in the mitochondrial depolarization, reflected by increase in percentage of depolarized cells (depolarized-live + depolarized-dead cells). An increase in depolarization from 9.57 ± 5.31% in the untreated control cells to 54.07 ± 2.10% and 66.21 ± 7.64% in the presence of 8.0 μM and 12.0 μM of 5′-Br was observed, respectively (Fig. 3A). Cells treated with 40.0 μM of z-VAD-FMK prior to addition of 8.0 μM of the compound resulted in only ~27% recovery of depolarization, suggesting that 5′-Br-induced disruption of mitochondria transmembrane potential is mostly caspase-independent. 5′-Br induced a time-dependent increase in the percentages of depolarized cells. A significant change in the mitochondria membrane potential was evident after incubation with 8.0 μM of the compound for 8 hr (25.00 ± 5.09%) and reached the peak value (55.50 ± 5.94%) after 20 hr (Fig. 3B). These results indicate that 5′-Br induces change in mitochondrial membrane potential in both dose and time dependent manner. 5′-Br-induced disruption of mitochondrial transmembrane potential interferes with ATP synthesis as shown by time dependent decrease in the relative levels of cellular ATP (Fig. 3C). The mean relative level of ATP decreased to 58.30 ± 6.7% after 24 hr.

Further, cytosolic cytochrome *c* was increased proportionally to 5′-Br concentration (Fig. 3D). The levels of cytochrome *c* that remained in the mitochondria of treated HL-60 cells decreased concomitantly (Fig. 3D). Detectable increase in the cytosolic cytochrome c was seen as early as 12 hr after incubating HL-60 with

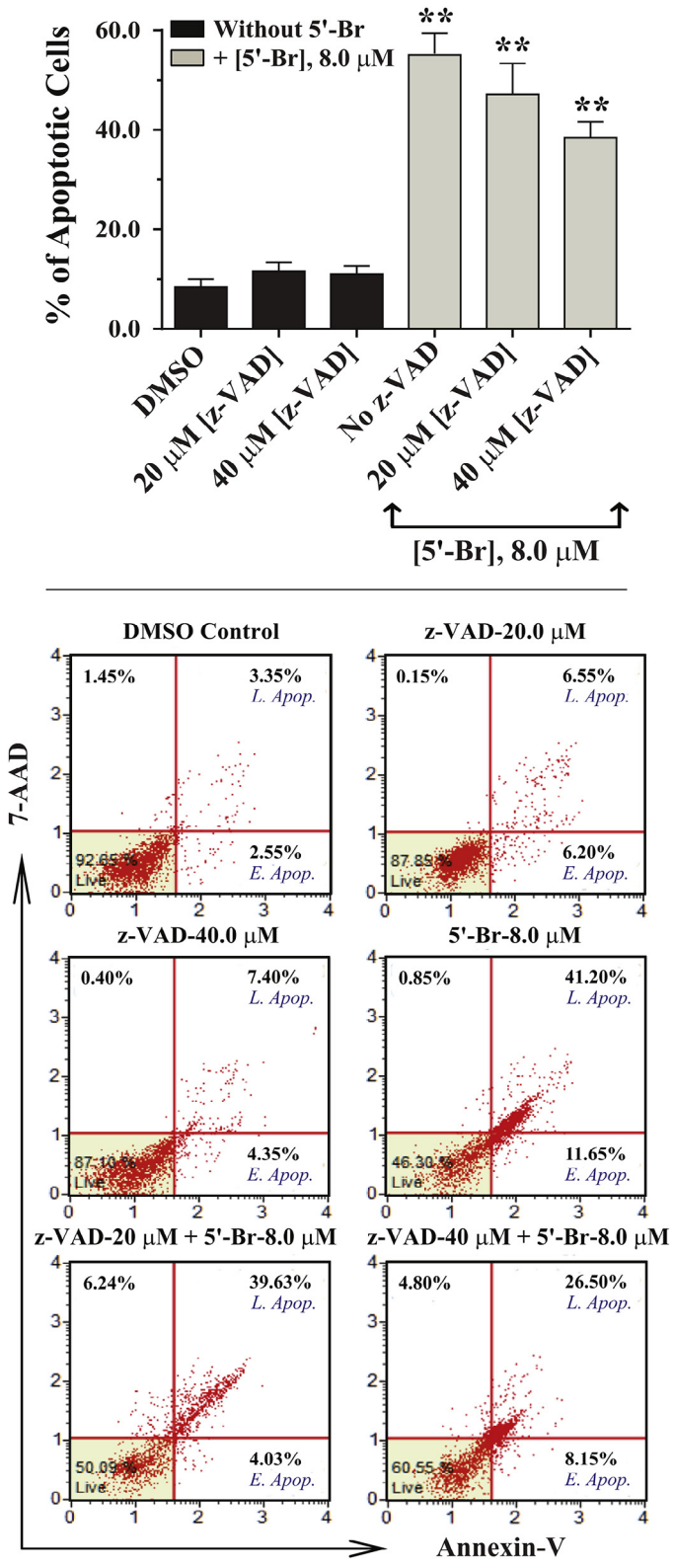

Fig. 2. Apoptosis induced by 5′-Br in HL-60 cells is partially dependent on caspase activation. z-VAD-FMK was able to partially rescue (31%) apoptotic cells. Bottom panel shows scatter plots representing one flow cytometry experiment. The graph represents the summary mean percentages ± SD of apoptosis (early and late apoptosis) of three independent experiments. (**) For values that are significantly different from untreated control ($p < 0.05$).

8.0 μM of 5′-Br (Supplementary Fig. S3A). However, the leakage of cytochrome c to the cytosol was not significantly inhibited by z-VAD-FMK, suggesting that its triggered release from mitochondria is independent of activation of caspase (Supplementary Fig. S3B). The release of cytochrome c coincides with the demonstrated 5′-Br dose and time dependency disturbance of mitochondrial functions and induction of apoptosis.

Expression and function of Bcl-2 protein are modulated by 5′-Br

Exposure of HL-60 cells to 5′-Br decreased the expression levels of the antiapoptotic protein Bcl-2 in a dose dependent manner (Fig. 4A and 4B). But there was an increase in phosphorylated forms of Bcl-2. However, the amount of the proapoptotic proteins Bax and Bak remains unchanged under the same treatment conditions. Also, the antiapoptotic Bcl-X_L protein levels did not change in the presence of 5′-Br (Fig. 4A).

Semi-quantitative RT-PCR results indicate that decreased level of Bcl-2 protein is due to the effect on gene expression rather than its post-translational degradation. Relative expression level of Bcl-2 was suppressed by a magnitude of ~6-fold in cells treated with 8.0 μM 5′-Br (Fig. 4C).

To monitor the effect of 5′-Br-induced hyperphosphorylation of Bcl-2 on its association with Bax, the Bax complex was immunoprecipitated from treated cells at different doses and the level of co-immunoprecipitated Bcl-2 in each complex was determined. As shown in Fig. 4D, the level of Bcl-2 co-immunoprecipitated with Bax from treated cells was significantly lower. The reciprocal immunoprecipitation experiment, under similar treatment conditions using an anti-Bcl-2 antibody, also showed a substantial concentration dependent reduction in the level of the co-immunoprecipitated Bax in treated cells (Fig. 4D). The association between Bcl-2 and Bax was dependent on the dose of 5′-Br and coincided with dose dependent hyperphosphorylation of Bcl-2 (Fig. 4A).

5′-Br induces cell cycle arrest in the G0/G1 phase by modulating the expression of regulatory proteins

When cells were treated with increasing concentrations of 5′-Br for 24 hr, a dose dependent cell cycle arrest at G0/G1 phase was evident with concomitant decrease in the S and G2/M phases. After treatment with 12.0 μM 5′-Br, cell population in G0/G1 phase increased by ~60%, whereas cells in G2/M and S phase were decreased by ~77% and ~36 % respectively (Fig. 5A). The cell cycle arrest was time dependent as exhibited by maximum response observed at 48 hr with ~54% increase in G0/G1 cell population (Supplementary Fig. S4). Change in cell population at different stages was accompanied by the change in the level of associated regulatory proteins. Cyclins D1 and D2 were found decreased along with cyclin dependent kinases, CDK2 and CDK4 but cyclin D3, cyclin E and CDK6 were not significantly affected by 5′-Br treatment (Fig. 5B). The expression of total Rb protein remained almost unchanged, while the phosphorylated-Rb significantly decreased in a dose dependent fashion (Fig. 5C). Expression of CDK inhibitors was found modulated as exhibited by increase in p21 levels (Fig. 5D).

Cyclin dependent kinase activity is inhibited by 5′-Br

In cell-free system, CDK2 and CDK4 were immunoprecipitated, and their activity was measured using histone H1 (for CDK2) or GST–Rb fusion protein (for CDK4) as substrates in the presence of [γ-^{32}P] ATP. *In vitro*, 5′-Br was able to inhibit both CDK2 (Fig. 6A) and CDK4 (Fig. 6B) with an approximate IC_{50} of ~6.48 ± 0.32 μM and ~4.85 ± 0.45 μM, respectively. The kinase activities of both CDK2 and CDK4 were inhibited in a dose dependent manner, and >95% of the substrates phosphorylation was observed after incubation with

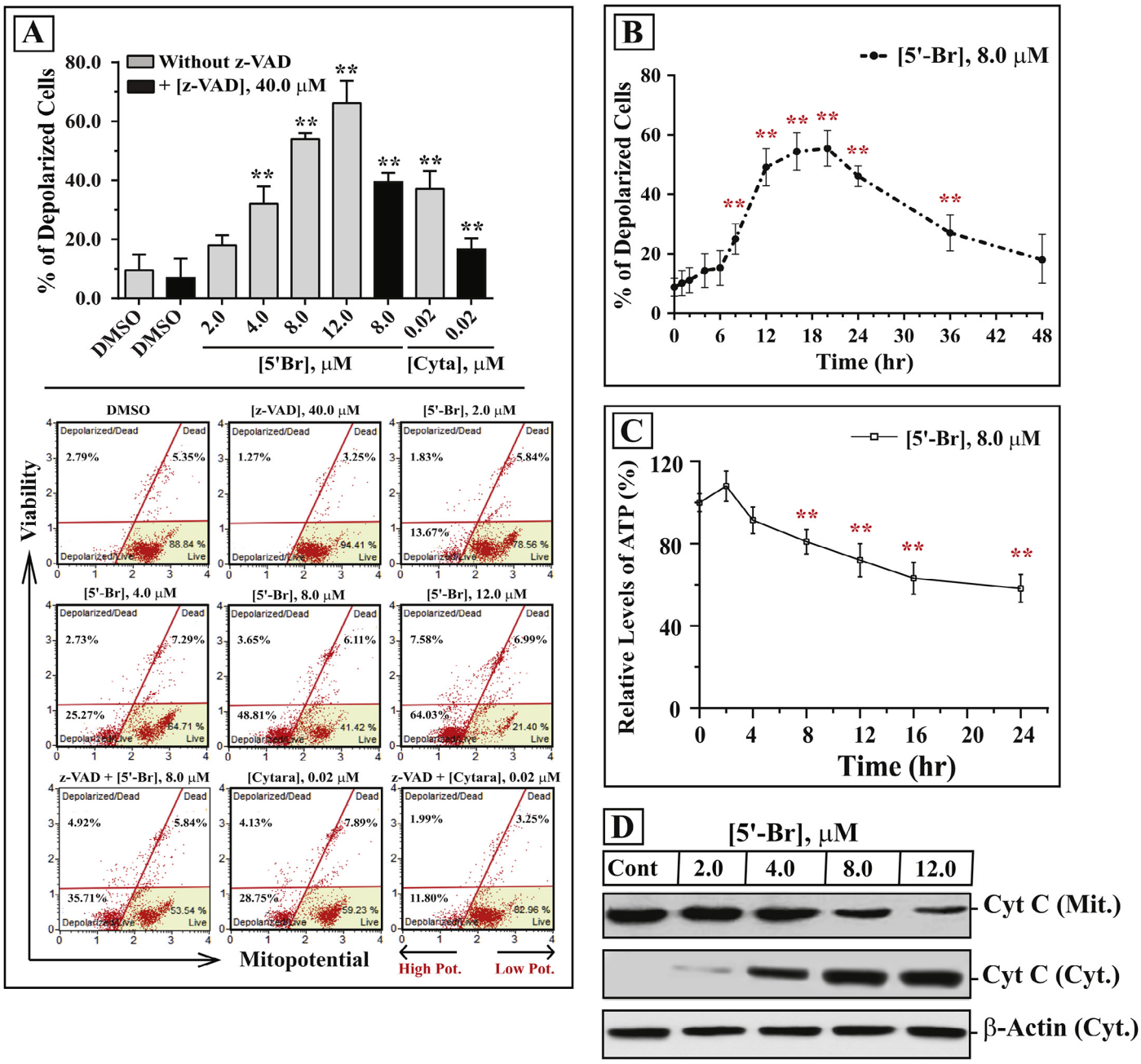

Fig. 3. 5′-Br induces dysfunctioning of mitochondria in HL-60 cells that is mostly independent from activation of caspases. (A) HL-60 cells were treated with varying concentrations of 5′-Br (0.0–12.0 μM) or 0.02 μM cytarabine in the presence and absence of 40 μM z-VAD-FMK for 12 hr. The scatter plots showing the percentages of live and dead depolarized cells are indicated for one experiment. The bar graph represents the mean percentages ± SD of total number of depolarized cells. (B) Peak depolarization effect of 5′-Br was observed at 20 hr treatment: HL-60 cells were exposed to 8.0 μM 5′-Br for increasing intervals and depolarization was assessed as described. (C) 5′-Br causes decrease in ATP levels: HL-60 cells were exposed to 8.0 μM 5′-Br for increasing periods and the level of ATP, relative to the untreated control, was determined as described. All the data shown represent the mean ± SD of three independent experiments. (**) For values that are significantly different from the proper control. (D) 5′-Br causes releases of cytochrome C in the cytosol: Immunoblot studies show mitochondrial (Mit., 30 μg fraction) cytochrome c levels decreased and cytosolic (Cyt., 50 μg fraction) levels increased in response to 5-Br treatment.

12.0 μM of 5′-Br (Fig. 6C and 6D). The inhibitory activity of 5′-Br was found to be time dependent with complete inhibition observed at 48 hr (Supplementary Fig. S5A and S5B).

Discussion

In the present study, we aim to analyze possible modes of action of a novel isoindigo compound (5′-Br) in human promyelocytic leukemia cells. We provide evidence that suggests involvement of apoptosis, mitochondrial dysfunction and cell cycle regulation as potential mechanisms. The antitumor properties of isoindigo derivatives have been studied with respect to apoptosis and cell cycle arrest (reviewed in Ref. 27). Indirubins and isoindigos appear to induce different cell death mechanism(s) that is determined by their structures. For 5′-Br-induced cell death, apoptosis seems to be the primary mechanism. This is supported by the following findings: first, 5′-Br-treated HL-60 cells showed the morphological aspects associated with early and late apoptotic events. Second, 5′-Br induced activation of the initiator caspases (-2, -8, and -9) and terminal caspases (-3 and -6). Third, 5′-Br caused cleavage of PARP, condensation of

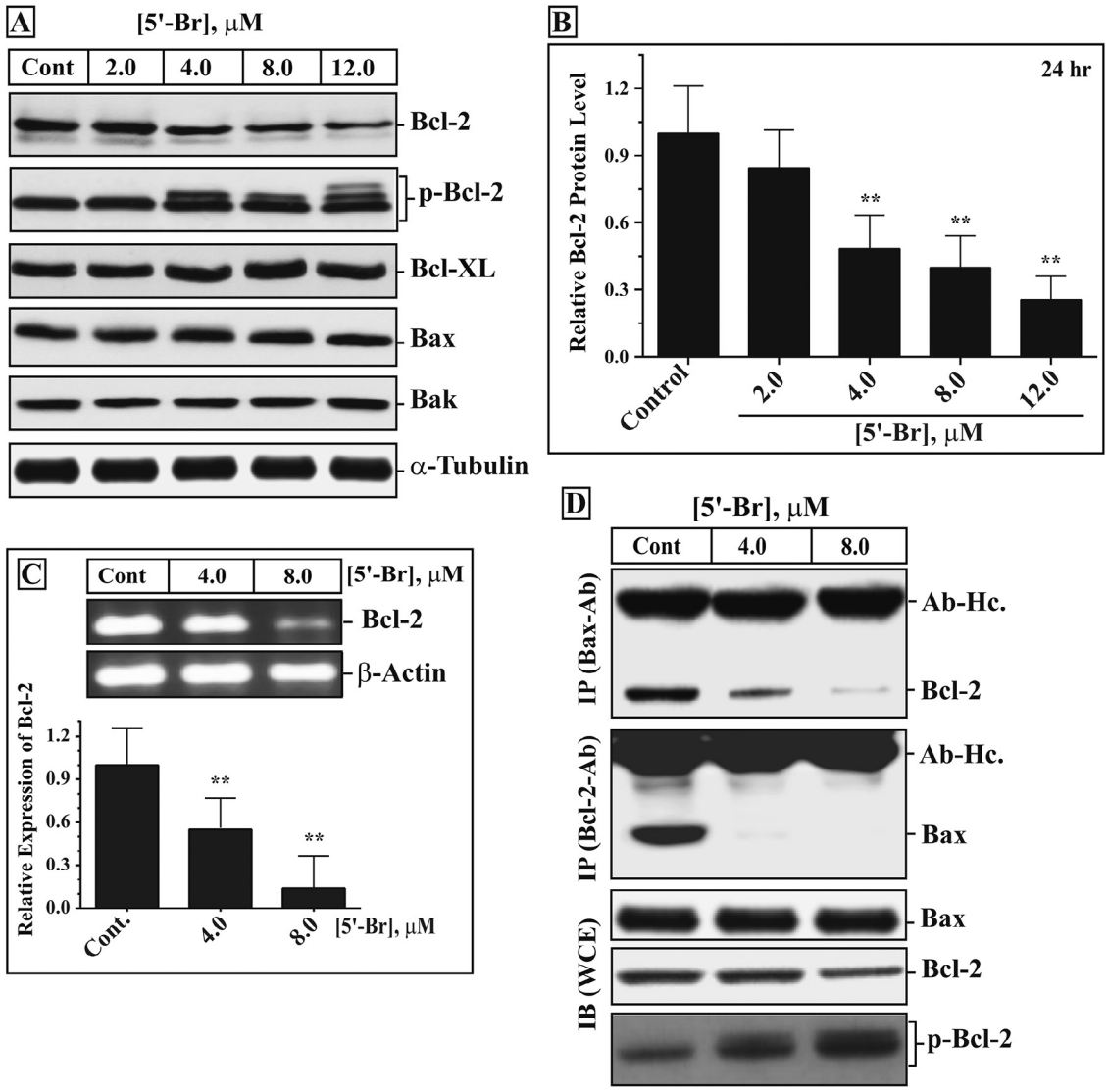

Fig. 4. 5′-Br modulates the expression and phosphorylation of Bcl-2, and its association with Bax. (A) 50 μg protein lysates, from HL-60 cells treated with increasing concentrations of 5′-Br, were immunoblotted with antibodies against Bcl-2, phospho-Bcl-2, Bcl-X_L, Bax, Bak and α-tubulin. Cont: DMSO treated control. (B) Densitometric scanning for the intensity levels of Bcl-2 (relative to untreated control), obtained from Western blotting of the protein in HL-60 cells treated with different concentrations of 5′-Br for 24 hr show decrease in levels of BCl-2 protein. The values represent the mean relative band densities ± SD of two independent experiments. (C) Semi-quantitative RT-PCR for *Bcl-2* mRNA obtained from untreated or treated cells with 5′-Br for 24 hr show a decrease in Bcl-2 mRNA levels. The densities of visualized bands (from three independent trials) were quantitated and the values were normalized to *β-actin* intensity levels. (**) For values that are significantly different from untreated control. (D) Bax or Bcl-2 were immunoprecipitated from whole cell lysates (300 μg), obtained from untreated and treated HL-60 with 5′-Br, and the presence of Bcl-2 or Bax in these complexes (IP) was visualized by Western blot analysis. The heavy chain of Bax and Bcl-2 antibodies (Ab-Hc) are also shown. Immunoblotting (IB) for Bcl-2, Box and phosho-Bcl-2 from 50 μg protein of the whole cell extracts (WCE) are shown to validate that the reduced amounts of coimmunoprecipitated Bcl-2 or Bax are due to loss of their protein–protein interactions, rather than variations in the protein levels.

chromatin material and fragmentation of nuclei in apoptotic HL-60 cells. Finally, 5′-Br caused depolarization of mitochondria (loss of $\Delta\Psi_m$) and caused the release of cytochrome *c* into the cytoplasm in a dose and time dependent manner, a characteristic for numerous stimuli that cause apoptosis *via* the intrinsic pathway involving mitochondria [14,28]. These evidence suggest involvement of apoptotic pathway in the mode of action of 5′-Br. Similar to HL-60 cells, 5′-Br induced apoptosis and activation of caspase-3 in K562, THP-1, HepG2, MCF-7, Caco-2 cell lines (Supplementary Fig. S6).

We further analyzed the depolarization of cells in response to 5′-Br to establish the involvement of mitochondrial dysfunction. Involvement of mitochondrial dysfunction was evident by the increase in number of depolarized cells in a dose and time dependent manner. However, our findings that z-VAD-FMK only partially rescued 5′-Br-treated cells from apoptosis and change in the mitochondria transmembrane potential ($\Delta\Psi_m$) suggest the involvement of caspase-dependent and caspase-independent pathways of cell death. Interestingly, the presence of z-VAD-FMK also did not inhibit ATP depletion (Supplementary Fig. S7), suggesting that the 5′-Br-induced dysfunctioning of the mitochondria in HL-60 cells is independent of caspase activation.

Since the activity of the Bcl-2 family proteins can be affected in cancer cells or modulated upon exposure to chemotherapeutic drugs, we have investigated the contribution of the major players in this family. We found that 5′-Br treatment resulted in a substantial decrease in expression of Bcl-2, while the levels of Bax, Bak and Bcl-xL were not affected. An increase in the ratio of Bax/Bcl-2 or Bak/Bcl-x_L stimulates the proapoptotic proteins Bax and Bak to form channels in the outer mitochondria membrane allowing cytochrome c to escape into the cytosol. The cytosolic cytochrome c will

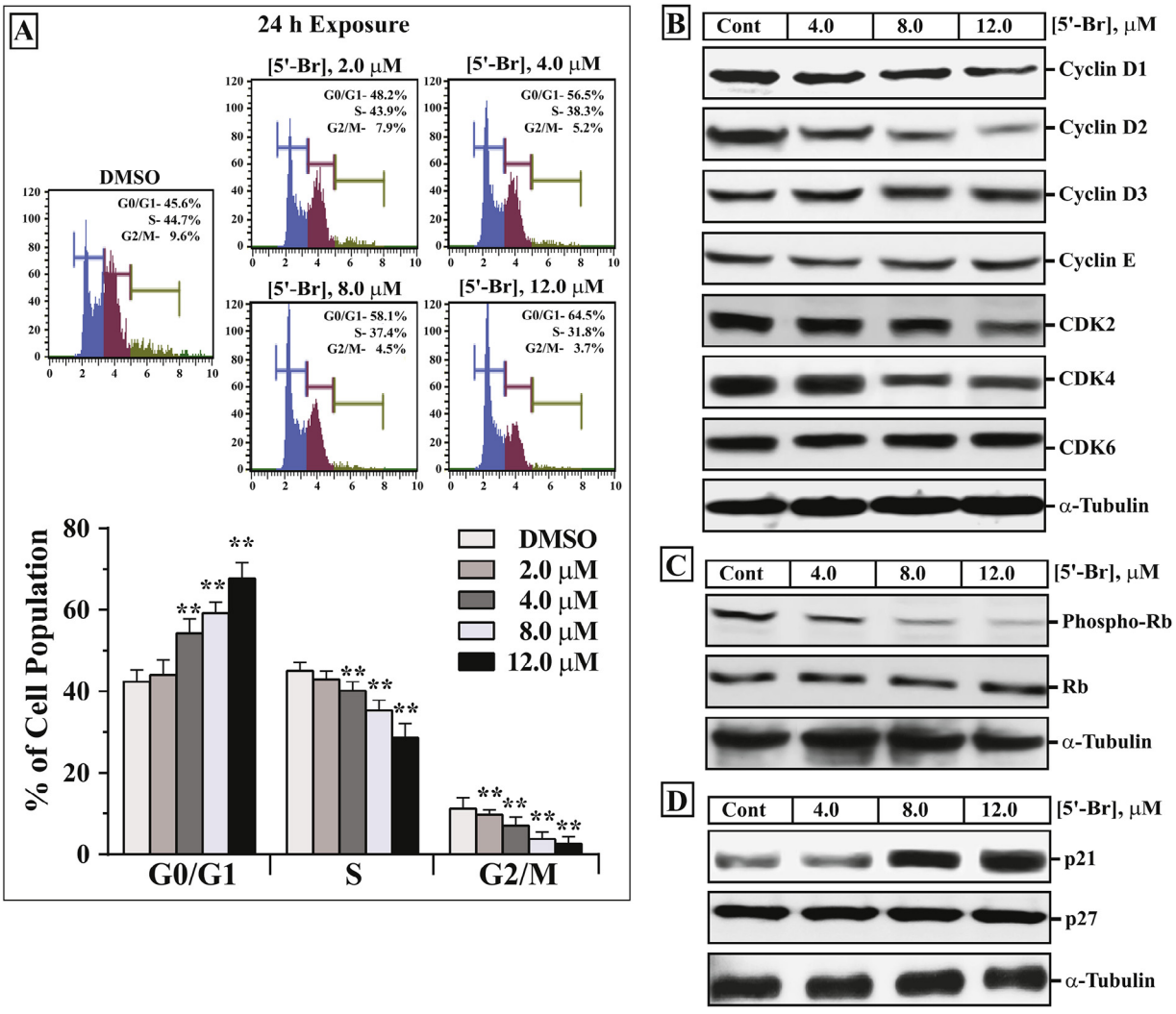

Fig. 5. 5′-Br induces a cell cycle arrest at G0/G1 phase in HL-60 cells. (A) In response to 5′-Br treatment an increase in the cell population at G1/G0 phase is observed represented by blue peak. Bottom panel shows bar graph representing quantified values of the flow cytometry data. Data shown are representative of one experiment. The graphs show the mean ± SD of the three independent cell cycle experiments. (**) For values that are significantly different from the untreated control. (B) HL60 cells were treated with increased concentrations of 5′-Br (2.0–12.0 μM) for 24 hr, then 50 μg of whole cell lysate was analyzed by Western blotting with antibodies against cyclins (D1, D2, D3 and E) and CDKs (CDK2, 4 and 6), (C) Rb and phospho-Rb, (D) and p21 and p27. The immunoblots shown are representations of two independent experiments. The same membranes were also probed with an antibody against α-tubulin as loading controls. (For interpretation of the references to color in this figure legend, the reader is referred to the web version of this article.)

bind and activate Apaf-1-caspase-9 apoptosome, leading to activation of caspase-3 [28]. Our data support this mechanism as evidenced by release of cytochrome c in the cytosol. These results may be responsible for the concomitant execution of apoptosis that we observed.

Our results show that 5′-Br is able to inactivate Bcl-2 *via* expression and hyperphosphorylation control. Activated caspases can cleave Bcl-2, generating an inactive form of the protein [29]. In addition, down-regulation of *Bcl-2* mRNA or Bcl-2 protein have been observed after treatment with different anticancer drugs [30,31]. In 5′-Br-induced apoptosis, the total Bcl-2 levels are decreased, suggesting that caspase-dependent cleavage, ubiquitin-directed degradation of the protein or alterations of mRNA levels maybe be involved. Although the 5′-Br-dependent cleavage or degradation of Bcl-2 cannot be ruled out, we could not detect the presence of short form (23 kD) of protein in western blots or ubiquitinated form in Bcl-2 immunoprecipitates from 5′-Br treated cells (data not shown). The levels of *Bcl-2* mRNA were decreased in a dose dependent manner, suggesting that 5′-Br interferes with *Bcl-2* gene expression. The tumor suppressor protein p53 was reported to regulate Bcl-2 family proteins through transcription-dependent and -independent mechanisms [32]. However, 5′-Br-induced alteration of *Bcl-2* expression in HL-60 cells seems to be independent of p53, since these cells are deficient in functional p53 [33,34]. Phosphorylation of Bcl-2 has been demonstrated as a mechanism for modulating the activity of the protein [35]. Our results show that 5′-Br induces a dose dependent increase in Bcl-2 hyperphosphorylation that correlates with loss of its heterodimerization with Bax in the immunoprecipitated complex from HL-60 treated cells. These results are consistent with several previous reports showing hyperphosphorylation of Bcl-2 was induced by cytotoxic drugs and chemotherapeutics, *e.g. Vinca* alkaloids, paclitaxel, doxorubicin and etoposide [36–38].

Our results support that 5′-Br triggers the intrinsic mitochondrial pathway of apoptosis. However, we cannot rule out the potential involvement of extrinsic receptor pathway(s) of apoptosis in 5′-Br treated cells. The later possibility is supported by 5′-Br induced activation of caspase-8. However, whether activation of caspase-8 is involved in 5′-Br-induced apoptosis or consequent to activation of

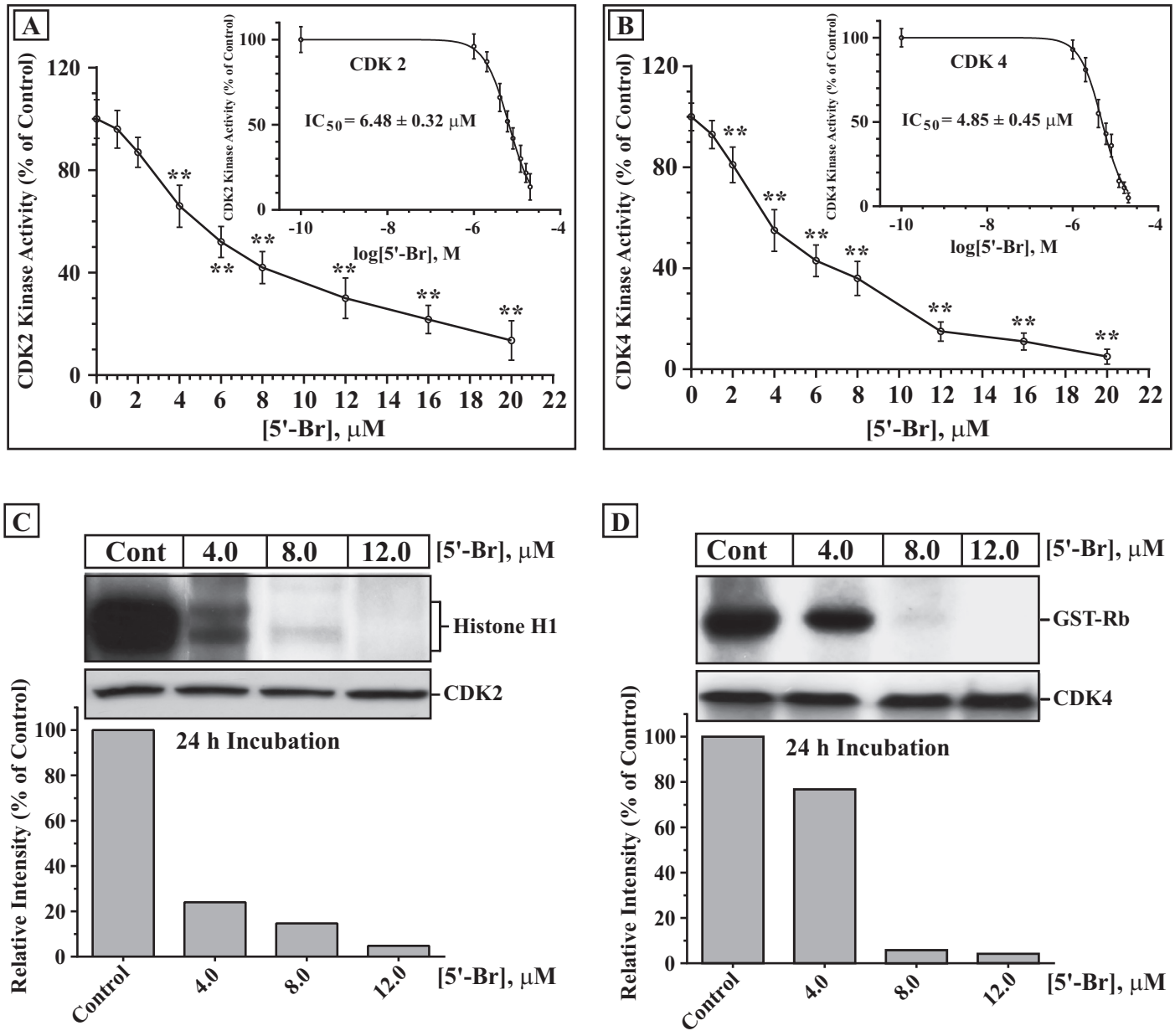

Fig. 6. 5′-Br inhibits the kinase activities of CDK2 and CDK4 in cell-free system and cultured HL-60 cells. CDK2 (A) and CDK4 (B) immunoprecipitated complexes were prepared from exponentially growing untreated cells, and reacted with [γ-^{32}P]ATP in the presence of histone H1 (for CDK2, A) and GST-Rb (for CDK4, B) substrates and increasing concentrations of 5′-Br as described under the methods. Quantification of the histone H1 and GST-Rb-phosphorylated forms was performed by densitometric analysis, and the IC_{50} was calculated using a non-linear regression analysis of GraphPad Prism 6. Data represent the means ± SD of three independent experiments. (**) For values that are significantly different from untreated control. (C and D) HL-60 cells were treated with various concentrations of 5′-Br (0.0–12.0 μM) for 24 hr. Total cell lysates were used for immunoprecipitation, and the kinase activities were assayed with histone H1 (C, for CDK2) and GST-Rb (D, for CDK4) as substrates. Data shown are representative of two independent experiments. The graphs represent the mean of the densitometric intensities of the visualized bands. The same immunoprecipitates were also immunoblotted with CDK2 and CDK4 to verify equal amounts of the desired CDK were present in each sample.

effector caspase-3 triggered by the release of cytochrome c remains to be investigated. Similarly, it is yet unclear whether 5′-Br-induced activation of the initiator caspase-2 is due to sequential activation of other caspases or response to potential direct action of the compound on damaging the DNA of HL-60 cells [39].

Several compounds similar to 5′-Br have been shown to arrest cell cycle, leading to cell death, by inhibiting CDKs and GSK-3β with varying degrees of potency [2–5,7–12,40]. We thus analyzed the effect of 5′-Br on cell cycle checkpoint regulation. Indirubin and several of its analogs exhibit their anticancer activity through modulating CDKs, which arrest cell cycle progression leading to apoptotic cell death [2–5,7–12,40]. Leclerc and coworkers have shown that the antiproliferative effect of indirubins is related to their ability to inhibit the kinase activity of GSK-3β, CDK1/cyclin B and CDK5/p25 [9]. Moon and coworkers [5] have synthesized novel indirubin analogs and shown that the antitumor activities are mediated by their ability to bind and inhibit the catalytic subunit of CDK2. Natura™, meisoindigo and other related compounds have been demonstrated to induce apoptosis in various cancer cell lines and inhibit the activity of CDK4, leading to cell cycle arrest at the G0/G1 phase [41]. Here we show that 5′-Br inhibits cell cycle progression and induces cell-cycle arrest in the G0/G1 phase in HL-60 cells both in a dose and time dependent manner. D-type cyclins (D1 and D2), CDK2 and CDK4 were significantly down-regulated leading to cell cycle arrest at G0/G1.

The CDK2 and CDK4 inhibition due to direct and indirect actions of 5′-Br could lead to hypophosphorylation of Rb in the treated cells. Though, the expression level of Rb is not affected, phosphorylated Rb levels decreased significantly in a dose dependent manner, indicating that 5′-Br can suppress the phosphorylation of this protein. Similar mechanism of inhibiting cell cycle progression to prevent cell proliferation has been reported earlier [20,42,43].

Our results show that 5′-Br induces a dose dependent increase in p21 which might lead to a reduction in the phosphorylation of Rb leading to cell cycle arrest at G0/G1 [44]. The expression of *p21* gene is controlled by p53-dependent and p53-independent mechanisms [45–47]. However, HL-60 and several other cancer cell lines are deficient in functional p53 [33,48,49], suggesting that 5′-Br-induced up-regulation of p21 is controlled *via* p53-independent mechanism.

The kinase activity of CDK2 and CDK4 was found inhibited *in vivo* in a dose and time-dependent manner in HL-60 treated cells. However, it is possible that 5′-Br inhibits the CDK activating kinases (CAKs) or activates the CDK-inactivating phosphatases, which are regulators for CDK function. Therefore, additional studies are needed to determine whether the inhibition of CAKs or activation of CDK-inactivating phosphatases contributes to the inhibition of the kinase activity of CDK2 and CDK4. In addition, CDK6 can also phosphorylate Rb within cells. The question of whether or not 5 ′-Br directly inhibits CDK6 activity remains to be answered. Furthermore, although down-regulation of D-type cyclins by 5′-Br suggests that it is the main causal effect for inhibiting the CDK4 kinase activity, we cannot rule out the possibility that the test compound may block cyclin D binding to CDK4, or binding of other cyclins to their specific CDKs, thereby inhibiting CDK4/cyclin D complex activity. Our results thus establish that 5′-Br arrests cell cycle at G0/G1 through its direct binding to the catalytic subunit of CDK2 and CDK4 and indirectly by modulating the expression of the two CDKs, cyclin D and p21.

The compound also inhibits G0/G1 cell cycle progression in K562, THP-1, HepG2 and MCF-7 (Supplementary Table S1). 5′-Br shows a dose-dependent accumulation of G2/M population in Caco-2 cells. This suggests that the targeted CDK/cyclin complexes by the compound may vary in different cancer cell lines (Supplementary Table S1). Caco-2 cells are heterogeneous, microsatellite stable [50] and have been reported to employ G2/M checkpoint regulation with increased p21 expression in response to dietary isothiocyanates [51]. Further mechanistic studies will provide insights into effect of 5′-Br in Caco-2 cells.

The potent inhibitory effects of 5′-Br against CDK2 and CDK4 prompted us to dock this compound into the binding pockets of both proteins and compare its optimal docked poses with the co-crystallized poses of corresponding potent ligands. Supplementary Fig. S8 compares how the potent CDK2 inhibitor, staurosporine, binds within CDK2 kinase binding pocket (PDB code: 4ERW, resolution 2.0 Å) with the way 5′-Br docks into the binding pocket of the same protein. Supplementary Fig. S8C and S8D suggests the 2-pyrrolidone of staurosporine and the 2-indolone of 5 ′-Br share similar hydrogen bonding pattern with the peptidic NH of Leu83 and the peptidic carbonyl of Glu81. Supplementary Fig. S9 compares how a potent CDK4 inhibitor (PDB code: 1PU501) binds within the X-ray crystal structure of CDK4 mimic CDK2 (PDB code: 1GIH, resolution 2.80 Å) with the way 5′-Br docks into the binding pocket of the same protein. Incidentally, inactive CDK2 monomer is closely homologous to CDK4 and therefore was used as a structural surrogate for CDK4 [52]. These docking studies suggest that 5′-Br may directly bind to the ATP binding site of the catalytic subunit of CDK2 and CDK4.

In conclusion, we have demonstrated that the antiproliferative activities of 5′-Br in HL-60 cells are primarily mediated by apoptosis, dysregulation of mitochondrial functions and arresting cell cycle at G0/G1 phase. These data, in addition to the previous finding that 5′-Br has a higher water solubility than the other reported isoindigos, and its ability to selectively induce apoptosis and cell cycle arrest in various cancer cell lines, but not in noncancerous cells at low exposure doses, strongly nominate this compound as a chemotherapeutic candidate. Therefore, detailed elucidation of the pathways and the respective targets of 5′-Br involved in apoptosis and cell cycle are critical for its potential application in cancer therapy. This study provides comprehensive analysis that paves the way for characterization of this novel molecule with potential anticancer effect.

Funding

This project is supported by a research grant from King Abdulaziz City for Science and Technology (KACST, Riyadh, Saudi Arabia; Grant number AT-34-136) for Saleh AM. El-Abadelah MM is supported by the Scientific Research Support Fund (SRSF/project number mph/1/6/2011, Amman, Jordan). Publication cost is supported by King Abdullah International Medical Research Center (KAIMRC, AT34/134) in Riyadh, Saudi Arabia.

Authors' contributions

AMS obtained the funds, designed the research project, supervised all experiments and drafted the manuscript; MME synthesized and characterized the 5′-Br molecule; MAA discussed results, planned and edited the manuscript; MOT performed the docking study; AN carried out viability and apoptosis assay and statistical analysis and SAAR performed the *in vitro* kinase assays. All authors reviewed the manuscript.

Conflict of interest

All the authors of this paper declare that they have no conflict of interest.

Appendix: Supplementary material

Supplementary data to this article can be found online at doi:10.1016/j.canlet.2015.03.013.

References

[1] B. Lowenberg, J.R. Downing, A. Burnett, Acute myeloid leukemia, N. Engl. J. Med. 341 (1999) 1051–1062.
[2] Z. Xiao, Y. Hao, B. Liu, L. Qian, Indirubin and meisoindigo in the treatment of chronic myelogenous leukemia in China, Leuk. Lymphoma 43 (2002) 1763–1768.
[3] X.M. Liu, L.G. Wang, H.Y. Li, X.J. Ji, Induction of differentiation and down-regulation of c-myb gene expression in ML-1 human myeloblastic leukemia cells by the clinically effective anti-leukemia agent meisoindigo, Biochem. Pharmacol. 51 (1996) 1545–1551.
[4] Z. Mingxin, L. Yan, W. Hongbo, Z. Jianhua, L. Hongyan, L. He, et al., The antitumor activity of meisoindigo against human colorectal cancer HT-29 cells in vitro and in vivo, J. Chemother. 20 (2008) 728–733.
[5] M.J. Moon, S.K. Lee, J.W. Lee, W.K. Song, S.W. Kim, J.I. Kim, et al., Synthesis and structure-activity relationships of novel indirubin derivatives as potent anti-proliferative agents with CDK2 inhibitory activities, Bioorg. Med. Chem. 14 (2006) 237–246.
[6] G.Y. Wu, J.Z. Liu, F.D. Fang, J. Zuo, Studies on the mechanism of indirubin action in the treatment of chronic granulocytic leukemia. V. Binding between indirubin and DNA and identification of the type of binding, Sci. Sin. [B.] 25 (1982) 1071–1079.
[7] D.J. Du, Q.T. Ceng, Effect of indirubin on the incorporation of isotope labeled precursors into nucleic acid and protein of tumor tissues, Chinese Trad. Herb Drugs 12 (1981) 406–409.
[8] X.J. Ji, F.R. Zhang, Y. Liu, Q.M. Gu, Studies on the antineoplastic action of N-methylisoindigotin, Yao Xue Xue Bao 20 (1985) 247–251.
[9] S. Leclerc, M. Garnier, R. Hoessel, D. Marko, J.A. Bibb, G.L. Snyder, et al., Indirubins inhibit glycogen synthase kinase-3 beta and CDK5/p25, two protein kinases involved in abnormal tau phosphorylation in Alzheimer's disease. A property common to most cyclin-dependent kinase inhibitors?, J. Biol. Chem. 276 (2001) 251–260.

[10] D. Marko, S. Schatzle, A. Friedel, A. Genzlinger, H. Zankl, L. Meijer, et al., Inhibition of cyclin-dependent kinase 1 (CDK1) by indirubin derivatives in human tumour cells, Br. J. Cancer 84 (2001) 283–289.
[11] M. Sassatelli, F. Bouchikhi, S. Messaoudi, F. Anizon, E. Debiton, C. Barthomeuf, et al., Synthesis and antiproliferative activities of diversely substituted glycosyl-isoindigo derivatives, Eur. J. Med. Chem. 41 (2006) 88–100.
[12] P. Zhao, Y. Li, G. Gao, S. Wang, Y. Yan, X. Zhan, et al., Design, synthesis and biological evaluation of N-alkyl or aryl substituted isoindigo derivatives as potential dual cyclin-dependent kinase 2 (CDK2)/glycogen synthase kinase 3beta (GSK-3beta) phosphorylation inhibitors, Eur. J. Med. Chem. 86 (2014) 165–174.
[13] J.J. Xu, X.M. Dai, H.L. Liu, W.J. Guo, J. Gao, C.H. Wang, et al., A novel 7-azaisoindigo derivative-induced cancer cell apoptosis and mitochondrial dysfunction mediated by oxidative stress, J. Appl. Toxicol. 31 (2011) 164–172.
[14] S.H. Kaufmann, W.C. Earnshaw, Induction of apoptosis by cancer chemotherapy, Exp. Cell Res. 256 (2000) 42–49.
[15] A. Saleh, S.M. Srinivasula, S. Acharya, R. Fishel, E.S. Alnemri, Cytochrome c and dATP-mediated oligomerization of Apaf-1 is a prerequisite for procaspase-9 activation, J. Biol. Chem. 274 (1999) 17941–17945.
[16] D. Schnerch, J. Yalcintepe, A. Schmidts, H. Becker, M. Follo, M. Engelhardt, et al., Cell cycle control in acute myeloid leukemia, Am. J. Cancer Res. 2 (2012) 508–528.
[17] C.J. Sherr, Cell cycle control and cancer, Harvey Lect. 96 (2000) 73–92.
[18] F. Ajchenbaum, K. Ando, J.A. DeCaprio, J.D. Griffin, Independent regulation of human D-type cyclin gene expression during G1 phase in primary human T lymphocytes, J. Biol. Chem. 268 (1993) 4113–4119.
[19] J. Gong, U. Bhatia, F. Traganos, Z. Darzynkiewicz, Expression of cyclins A, D2 and D3 in individual normal mitogen stimulated lymphocytes and in MOLT-4 leukemic cells analyzed by multiparameter flow cytometry, Leukemia 9 (1995) 893–899.
[20] H. Muller, K. Helin, The E2F transcription factors: key regulators of cell proliferation, Biochim. Biophys. Acta 1470 (2000) M1–M12.
[21] N.P. Pavletich, Mechanisms of cyclin-dependent kinase regulation: structures of Cdks, their cyclin activators, and Cip and INK4 inhibitors, J. Mol. Biol. 287 (1999) 821–828.
[22] A.M. Saleh, R.M. Al-As'ad, M.M. El-Abadelah, S.S. Sabri, J.A. Zahra, A.S. Alaskar, et al., Synthesis and biological evaluation of new pyridone-annelated isoindigos as anti-proliferative agents, Molecules 19 (2014) 13076–13092.
[23] A.M. Saleh, A. Aljada, S.A. Rizvi, A. Nasr, A.S. Alaskar, J.D. Williams, In vitro cytotoxicity of Artemisia vulgaris L. essential oil is mediated by a mitochondria-dependent apoptosis in HL-60 leukemic cell line, BMC Complement. Altern. Med. 14 (2014) 226.
[24] L. Li, H.J. Dai, M. Ye, S.L. Wang, X.J. Xiao, J. Zheng, et al., Lycorine induces cell-cycle arrest in the G0/G1 phase in K562 cells via HDAC inhibition, Cancer Cell Int. 12 (2012) 49.
[25] P.L. Miliani de Marval, E. Macias, R. Rounbehler, P. Sicinski, H. Kiyokawa, D.G. Johnson, et al., Lack of cyclin-dependent kinase 4 inhibits c-myc tumorigenic activities in epithelial tissues, Mol. Cell. Biol. 24 (2004) 7538–7547.
[26] M.R. Ramsey, J. Krishnamurthy, X.H. Pei, C. Torrice, W. Lin, D.R. Carrasco, et al., Expression of p16Ink4a compensates for p18Ink4c loss in cyclin-dependent kinase 4/6-dependent tumors and tissues, Cancer Res. 67 (2007) 4732–4741.
[27] Z. Xiao, Y. Wang, L. Lu, Z. Li, Z. Peng, Z. Han, et al., Anti-angiogenesis effects of meisoindigo on chronic myelogenous leukemia in vitro, Leuk. Res. 30 (2006) 54–59.
[28] W. Hu, J.J. Kavanagh, Anticancer therapy targeting the apoptotic pathway, Lancet Oncol. 4 (2003) 721–729.
[29] B. Fadeel, Z. Hassan, E. Hellstrom-Lindberg, J.I. Henter, S. Orrenius, B. Zhivotovsky, Cleavage of Bcl-2 is an early event in chemotherapy-induced apoptosis of human myeloid leukemia cells, Leukemia 13 (1999) 719–728.
[30] S. Bandyopadhyay, T.K. Sengupta, D.J. Fernandes, E.K. Spicer, Taxol- and okadaic acid-induced destabilization of bcl-2 mRNA is associated with decreased binding of proteins to a bcl-2 instability element, Biochem. Pharmacol. 66 (2003) 1151–1162.
[31] R.J. Lutz, Role of the BH3 (Bcl-2 homology 3) domain in the regulation of apoptosis and Bcl-2-related proteins, Biochem. Soc. Trans. 28 (2000) 51–56.
[32] M.T. Hemann, S.W. Lowe, The p53-Bcl-2 connection, Cell Death Differ. 13 (2006) 1256–1259.
[33] L.R. Livingstone, A. White, J. Sprouse, E. Livanos, T. Jacks, T.D. Tlsty, Altered cell cycle arrest and gene amplification potential accompany loss of wild-type p53, Cell 70 (1992) 923–935.
[34] K.H. Vousden, D.P. Lane, p53 in health and disease, Nat. Rev. Mol. Cell Biol. 8 (2007) 275–283.
[35] C.D. Scatena, Z.A. Stewart, D. Mays, L.J. Tang, C.J. Keefer, S.D. Leach, et al., Mitotic phosphorylation of Bcl-2 during normal cell cycle progression and Taxol-induced growth arrest, J. Biol. Chem. 273 (1998) 30777–30784.
[36] N. Azad, A.K. Iyer, A. Manosroi, L. Wang, Y. Rojanasakul, Superoxide-mediated proteasomal degradation of Bcl-2 determines cell susceptibility to Cr(VI)-induced apoptosis, Carcinogenesis 29 (2008) 1538–1545.
[37] S. Luanpitpong, P. Chanvorachote, U. Nimmannit, S.S. Leonard, C. Stehlik, L. Wang, et al., Mitochondrial superoxide mediates doxorubicin-induced keratinocyte apoptosis through oxidative modification of ERK and Bcl-2 ubiquitination, Biochem. Pharmacol. 83 (2012) 1643–1654.
[38] L. Wang, P. Chanvorachote, D. Toledo, C. Stehlik, R.R. Mercer, V. Castranova, et al., Peroxide is a key mediator of Bcl-2 down-regulation and apoptosis induction by cisplatin in human lung cancer cells, Mol. Pharmacol. 73 (2008) 119–127.
[39] S. Kumar, Caspase 2 in apoptosis, the DNA damage response and tumour suppression: enigma no more?, Nat. Rev. Cancer 9 (2009) 897–903.
[40] R. Hoessel, S. Leclerc, J.A. Endicott, M.E. Nobel, A. Lawrie, P. Tunnah, et al., Indirubin, the active constituent of a Chinese antileukaemia medicine, inhibits cyclin-dependent kinases, Nat. Cell Biol. 1 (1999) 60–67.
[41] L. Wang, X. Liu, R. Chen, Derivatives of isoindigo, indigo and indirubin and use in treating cancer. WO Patent. WO 03/051900 A1, 2003.
[42] J. Botz, K. Zerfass-Thome, D. Spitkovsky, H. Delius, B. Vogt, M. Eilers, et al., Cell cycle regulation of the murine cyclin E gene depends on an E2F binding site in the promoter, Mol. Cell. Biol. 16 (1996) 3401–3409.
[43] R.A. Weinberg, The retinoblastoma protein and cell cycle control, Cell 81 (1995) 323–330.
[44] Y. Taya, RB kinases and RB-binding proteins: new points of view, Trends Biochem. Sci. 22 (1997) 14–17.
[45] W.S. el-Deiry, J.W. Harper, P.M. O'Connor, V.E. Velculescu, C.E. Canman, J. Jackman, et al., WAF1/CIP1 is induced in p53-mediated G1 arrest and apoptosis, Cancer Res. 54 (1994) 1169–1174.
[46] W.S. el-Deiry, T. Tokino, V.E. Velculescu, D.B. Levy, R. Parsons, J.M. Trent, et al., WAF1, a potential mediator of p53 tumor suppression, Cell 75 (1993) 817–825.
[47] A.J. Levine, p53, the cellular gatekeeper for growth and division, Cell 88 (1997) 323–331.
[48] S.B. Parker, G. Eichele, P. Zhang, A. Rawls, A.T. Sands, A. Bradley, et al., p53-independent expression of p21Cip1 in muscle and other terminally differentiating cells, Science 267 (1995) 1024–1027.
[49] Y. Yin, M.A. Tainsky, F.Z. Bischoff, L.C. Strong, G.M. Wahl, Wild-type p53 restores cell cycle control and inhibits gene amplification in cells with mutant p53 alleles, Cell 70 (1992) 937–948.
[50] B. Youngblood, A. Noto, F. Porichis, R.S. Akondy, Z.M. Ndhlovu, J.W. Austin, et al., Cutting edge: prolonged exposure to HIV reinforces a poised epigenetic program for PD-1 expression in virus-specific CD8 T cells, J. Immunol. 191 (2013) 540–544.
[51] J.M. Visanji, S.J. Duthie, L. Pirie, D.G. Thompson, P.J. Padfield, Dietary isothiocyanates inhibit Caco-2 cell proliferation and induce G2/M phase cell cycle arrest, DNA damage, and G2/M checkpoint activation, J. Nutr. 134 (2004) 3121–3126.
[52] N. Kawanishi, T. Sugimoto, J. Shibata, K. Nakamura, K. Masutani, M. Ikuta, et al., Structure-based drug design of a highly potent CDK1,2,4,6 inhibitor with novel macrocyclic quinoxalin-2-one structure, Bioorg. Med. Chem. Lett. 16 (2006) 5122–5126.